Iranian Journal of Pathology | ISSN: 2345-3656

Allogenic Bone Graft Enriched by Periosteal Stem Cell and Growth Factors for Osteogenesis in Critical Size Bone Defect in Rabbit Model: Histopathological and Radiological Evaluation

Hadi Hassibi[1], Alireza Farsinejad[2], Shahriar Dabiri[3], Darioush Voosough[4], Abbas Mortezaeizadeh[3], Reza Kheirandish[5], Omid Azari[4*]

1. *Department of Veterinary Surgery, Shahid Bahonar University of Kerman, Kerman, Iran*
2. *Department of Hematology and Medical Laboratory Sciences, Faculty of Allied Medicine, Kerman University of Medical Science, Kerman, Iran*
3. *Pathology and stem cell Research Center, Department of Pathology, Kerman University of Medical Sciences, Kerman, Iran*
4. *Department of Clinical Sciences, Faculty of Veterinary Medicine, Shahid Bahonar University of Kerman, Kerman, Iran*
5. *Department of Pathobiology, Faculty of Veterinary Medicine, Shahid Bahnoar University of Kerman, Kerman, Iran*

KEYWORDS

Bone healing,
Growth factors,
Stem cell,
Allogeneic bone graft,
Rabbit

Scan to discover online

Main Subjects:
Bone & Soft tissue Pathology

Received 19 Jan 2019;
Accepted 09 April 2020;
Published Online 21 Apr 2020;

10.30699/ijp.2020.101715.2013

ABSTRACT

Background & Objective: This study aimed to investigate the effect of decellularized allogeneic bone graft enriched by periosteal stem cells (PSCs) and growth factors on the bone repair process in a rabbit model, which could be used in many orthopedic procedures.

Methods: In this experimental study, a critical size defect (CSD) (10 mm) was created in the radial diaphysis of 40 rabbits. In group A, the defect was left intact with no medical intervention. In group B, the defect was filled by a decellularized bone graft. In group C, the defect was implanted by a decellularized bone graft enriched with platelet growth factors. In group D, the defect was treated by a decellularized bone graft seeded by periosteal mesenchymal stem cells (MSCs). Also, in group E, the defect was filled by a decellularized bone graft enriched with platelet growth factors and periosteal MSCs. Radiological evaluation was done on the first day and then in the second, fourth, and eighth weeks after the operation. The specimens were harvested on the 28th and 56th postoperative days and evaluated for histopathological criteria.

Results: The radiologic and microscopic analysis of the healing process in bone defects of the treated groups (C, D, and E) revealed more advanced repair criteria than those of groups A and B significantly (P<0.05).

Conclusion: Based on this study, it appears that implantation of concentrated PSCs in combination with growth factors and allogeneic cortical bone graft is an effective therapy for the repair of large bone defects.

Corresponding Information: **Omid Azari**; Omid Azari, Department of Clinical Sciences, Faculty of Veterinary Medicine, Shahid Bahonar University of Kerman, Kerman, Iran. E mail: omidazari@uk.ac.ir Phone number: 09123185781

Introduction

Bone grafting is used for the treatment of several conditions that represent a great global burden, including critical size bone defects caused by trauma, tumor excision or chronic osteomyelitis, and nonunion and delayed union. Under the optimal environment, many bone fractures heal completely without fibrous scar tissue in the first 6 to 8 weeks (1). A nonunion fracture is known as a fracture that fails to heal and stops the process of fracture healing, in which the fracture gap fills with persistent fibrous tissue, woven bone, and cartilage. In this regard, nonunion fractures are divided into two categories of hypertrophic nonunion and atrophic nonunion (2, 3).

Moreover, a delayed union is defined as a fracture that fails to repair within an anticipated period (4). The normal time of fracture healing depends on the bone, type of fracture, fracture location, age of the patient, and type of fixation (5–7). Cases requiring surgical intervention typically heal via the endochondral ossification pathway, which is generally divided into four consecutives but overlapping phases: hematoma formation, soft callus formation, hard callus formation, and remodeling (8). Operative intervention is necessary to promote fracture union, and the current gold standard treatment is autografts (9). They have optimal osteoconductive, osteoinductive, and osteogenic properties.

As an alternative, allografts are widely available in various shapes and sizes. Allografts may be cancellous, cortical, or cortico-cancellous (10). Cortical bone grafts are used clinically in the repair of severely

comminuted diaphyseal fractures when the mechanical support of cortical bone is necessary for the rigid stabilization of the fracture (11). However, they place patients at risk for infections and rejection by the immune system (12,13). Because of the disease transmission and immune response, fresh bone allografts are seldom used. Decellularization of soft and hard connective tissues, such as bones, reduces or even eliminates the immunogenicity associated with allografts and, therefore, may be effective in enhancing the incorporation of these grafts (14–18). Recent progress in the fields of tissue engineering has offered the use of scaffolds, growth factors, and stem cells for the repair of segmental bone defects. Mesenchymal stem cells (MSCs) can be harvested from several tissues and organs, such as the umbilical cord blood, bone marrow, periosteum, synovium, and adipose tissue (19).

Bone consists of separate inner endosteal and outer periosteal compartments, each with distinct contributions to bone physiology and each maintaining separate pools of cells owing to the physical separation by the bone cortex (20). The periosteum is a tough and vascular connective tissue membrane consisting of two layers, i.e., the inner layer (termed osteogenic layer) and the thick outer layer (called the fibrous layer). The osteogenic layer, which is close to the surface of the bone, contains more cellular components than the outer layer. The cellular components of the periosteum generally include cells that are responsible for bone remodeling and their precursor cells. Periosteal stem cell (PSC) implantation is a biological method for the treatment of large and full-thickness bone (21).

Growth factors are protein signaling agents, which are pleiotropic, causing multiple biological effects; they are expressed during different phases of bone repair. Some growth factors, such as fibroblast growth factor (FGF), bone morphogenetic proteins (BMPs), insulin-like growth factors (IGFs), platelet-derived growth factor (PDGF), transforming growth factor-beta (TGF-beta) and vascular endothelial growth factor (VEGF), are capable of promoting vascularization and osteogenesis. Many of these factors are known to play a role in the differentiation of mesenchymal progenitor cells to specific lineages such as chondroblast and osteoblast; thus, they can be useful in improving the healing processes (22–24). Therefore, the potentiality of allograft transplantation with PSC and growth factors needs to be investigated further for general application.

This study was designed to evaluate the bone formation properties of an allogeneic demineralized cortical bone scaffold seeded with allogeneic PSCs and enriched by a xenogeneic growth factor in a critical-sized bone defect model in rabbits.

Materials and Methods

Preparation of Decellularized Bone Scaffolds

Cylindrical and cortical bone grafts were harvested from the diaphysis region of the radius of the New Zealand rabbit. The bones were washed with a high-velocity stream of water to remove the marrow from the pore spaces and then for 1 hr in phosphate-buffered saline (PBS) (Gibco, Paisley, United Kingdom) with 0.1% ethylenediaminetetraacetic acid (EDTA) (Merck, Darmstadt, Germany) at room temperature. This step was followed by sequential washes in hypotonic buffer (10 mM Tris (Sigma-Aldrich, Steinheim, Germany); 0.1% EDTA, overnight at 4°C), detergent (10 mM Tris, 0.5% sodium dodecyl sulfate (SDS) (Merck, Darmstadt, Germany), for 24 hr at room temperature), and enzymatic solution (50 U/mL DNAse, 1 U/mL RNAse, 10 mM (Sigma-Aldrich, Steinheim, Germany) Tris, for 3–6 hr at 37°C) to remove any remaining cellular material. After each step, the scaffolds were rinsed with PBS for 1 hr. After SDS treatment, several washes (≥ 7) were performed until no more bubbles (indicating the presence of detergent) were seen in the PBS during washing. At the end of the process, decellularized bone plugs were rinsed in PBS, freeze-dried, and cut to 9 mm long cylinders. Scaffolds were sterilized in 70% ethanol for 1 hr and incubated in culture medium overnight before seeding cells.

Preparation of Periosteal Mesenchymal Stem Cells

In order to obtain allogeneic periosteum, a New Zealand rabbit (outside of this study) became anesthetized and prepared for operation. The radius was approached, and a 0.5 × 1 cm piece of periosteum was harvested from the bone with a periosteal elevator under the sterile condition and cultured in a basic culture medium (DMEM-F12 Gibco, Paisley, UK). In order to separate the stem cells, the periosteum was washed with phosphated buffer and cut into several pieces with a sterile surgical blade. The pieces were placed in a 2% type 1 collagenase (SERVA, Heidelberg, Germany) solution for 30 min. The solution was then passed through a 122 µ Millipore filter (Jet biofilm, Beijing, China). The equal volume of PBS was then added to the solution, and the resulting mixture was centrifuged for 1 min at 1200 rpm. Then, 5000 cells per square centimeter were cultured from a 75 cm square flask (SPL, Pyeongtaek, South Korea). The culture medium of these cells was DMEM-F12, containing 12% cow serum, penicillin (Gibco, Paisley, UK), and acetaminophen. The plate containing cells was transferred to a 37-degree incubator containing 5% CO_2, and after the appearance of spiky colonies, the medium was replaced. Third-passage cells were used in the subsequent experiments.

Growth Factors Preparation

Growth stimulants were obtained from human platelets. For this purpose, a platelet concentrate bag from the Iranian Blood Transfusion Organization was received. The content of the bag was poured into a 50 mL falcon (SPL, Pyeongtaek, South Korea) under the sterile condition and centrifuged at 3500 rpm for 15 min. Platelet sediments, along with a small amount of plasma,

were kept in the 50 mL flask, and the supernatant solution was discarded. By adding 1 mL of human thrombin (Sigma-Aldrich, Steinheim, Germany) and 10% calcium chloride (Merck, Darmstadt, Germany), the platelets were activated. In the next step, the platelets' extract was isolated by centrifugation and used as a source of platelet growth factors.

Animals and Surgical Procedure

Forty New Zealand white rabbits (eight months old, of both sexes, weighing 2.0 ± 0.5 kg) were housed in separate cages, fed a standard diet and allowed to move freely during the study. All the procedures were conducted in accordance with the European Community guidelines for laboratory animals and under the supervision of the Ethics Committee of the Faculty of Veterinary Medicine, Shahid Bahonar University of Kerman. All surgical procedures were carried out in the Teaching Hospital of Veterinary Faculty of the Shahid Bahonar University of Kerman.

The scaffold, growth factors, and stem cell were prepared in the pathology and Stem Cell Research Center of the Afzalipour Medical Sciences University of Kerman. The animals were randomly divided into five equal groups for scaffold implantation: Group A: The critical size bone defect was left as such (untreated) for control study (n=8); Group B: The decellularized bone graft only group (n=8); Group C: The graft enriched by growth factors group (n=8); Group D: The decellularized bone graft seeded by PSCs group (n=8); and Group E: The decellularized bone graft seeded with PSCs and growth factors (n=8). All the animals were anesthetized by intramuscular administration of 40 mg/kg ketamine hydrochloride (Alfasan International, Woerden, the Netherlands) and 5 mg/kg xylazine (Alfasan International, Woerden, the Netherlands).

The right forelimb was prepared aseptically for operation. A 5 cm incision was made craniomedially of the forelimb, and the radius was exposed through a longitudinal incision by gentle retraction of the muscles. A 10 mm segmental defect was created by a surgical saw in the diaphysis of the radius as a critical size defect (CSD) (25). The graft, according to the groups, was placed in the defect and stabilized by an interfragmentary wire method. The ulna was left intact for mechanical stability. After implantation, muscle, fascia, and skin were separately closed over the defect. Intraoperative anteroposterior (craniocaudal) and mediolateral radiographs were used to confirm the adequate placement of hardware and bone alignment. The forelimb was supported by a splint for two weeks. All rabbits received an intramuscular injection of antibiotic Pantrisol (each mL solution contains 40 mg trimethoprim and 200 mg sulfamethoxazole, Pantex Co., Holland) (30 mg/kg BW, bid, IM) intraoperatively and four days after surgery. Postoperative pain reduction was achieved by administering tramadol (5 mg/kg, Darou Pakhsh Pharma. Chem. Co. Tehran, Iran) subcutaneously for two days.

The wound was evaluated daily for the duration of the study, including signs of swelling and discoloration. The dietary habits and daily activity were also observed to discern any possible abnormalities resulting from the implantation. All rabbits were sacrificed four and eight weeks after surgery for gross observation and histological analyses.

Radiological Evaluation

To evaluate bone formation, proximal and distal unions, and remodeling of the defect, radiographs of each forelimb were taken postoperatively on the first day and then in the second, fourth, and eighth weeks post-surgery. The assessment of new bone formation and remodeling was based on the modified Lane and Sandhu radiological scoring system (26). Two radiologists blindly assessed the radiological scores; the score for new bone formation was determined as follows: (0), no new bone formation; (1), less than 25% new bone formation; (2), 25%–50% new bone formation; (3), 50%–75% new bone formation; or (4), more than 75% new bone formation. The score assigned to the assessment of union was as follows: (0), nonunion; (1), possible union; or (2), radiographic union. The proximal and distal unions of the bone graft were separately evaluated. The remodeling score assigned was as follows: (0), no evidence of remodeling; (2), intramedullary remodeling; or (4), cortical remodeling. The maximum number of points, which could be achieved, was 10 for each reconstructed bone.

Histopathological Evaluation

The right forelimb was harvested and dissected free of soft tissues. Forty specimens from the bone graft sites of the radius were successfully fixed with 10% formalin. The formalin-fixed bone samples were decalcified in a 15% buffered formic acid solution and embedded in paraffin. Five-micron thick sections were cut from the centers of each specimen, then prepared and stained with hematoxylin and eosin (H&E), as well as toluidine blue and Masson's trichrome, and observed under light microscopy (Olympus BX51, Olympus Optical Co., Tokyo, Japan). The samples were blindly apprised and scored by two pathologists based on Emery's scoring system. When the gap was empty, the score was equal to (0); if the gap was filled with fibrous tissue only, the score was equal to (1); with more fibrous tissue than the fibrocartilage, the score was equal to (2); with more fibrocartilage than the fibrous tissue, the score was equal to (3); fibrocartilage only, the score was equal to (4); with more fibrocartilage than the bone, the score was equal to (5); with more bone than the fibrocartilage, the score was equal to (6); and filled only with bone, the score was equal to (7) (27,28). The host response to the scaffold was also evaluated by an experienced pathologist regarding the cellular infiltration, presence of multinucleate giant cells, vascularity, connective tissue organization, encapsulation, and degradation.

Statistical Analysis

In the present study, all data were presented as median and ranged by SPSS version 17 for windows (SPSS Inc., Chicago, Ill., USA). The radiological and histopathological data were compared by Kruskal-

Wallis, non-parametric analysis of variance (ANOVA), when P-values were found to be less than 0.05, then pairwise group comparisons were performed by the Mann–Whitney U test.

Results

The wounds healed completely after one week, and the rabbits were noted to regain full movement within two weeks. All the rabbits survived with normal behavior. No complications, such as infection or necrosis, were recorded prior to sacrifice.

Radiographic findings

In week 2

The analysis of radiological data showed that there was a significant difference in bone formation of Group A (blank group), in comparison with Group B, and all treated groups (C, D and E; $P<0.05$), and there was no significant difference between the treated groups ($P>0.05$; Table 1)

Also, the radiological findings depicted that there was no evidence of proximal and distal bone unity and remodeling in any control and treated groups. Remodeling was not found in either group on the 14th day post-surgery (Tables 2 and 3).

Table 1. Radiological findings for bone formation at various postoperative intervals

Median (Range)			
Groups	Week 2	Week 4	Week 8
A	0 (0-1)	1 (1-1)[@#]	3 (3-3)[@]
B	1 (1-1)[*]	1 (1-1)[@#]	3 (3-3)[@]
C	1 (1-1)[*]	1 (1-2)[@#]	3 (3-4)
D	1 (1-1)[*]	2 (1-2)	3.5 (3-4)
E	1 (1-2)[*]	2 (2-2)	4 (3-4)

- Symbol (*) shows significant difference in comparison with group A ($P<0.05$), at week 2.
- Symbol ([@]) shows significant difference in comparison with group E ($P<0.05$), at weeks 4 & 8.
- Symbol ([#]) shows significant difference in comparison with group D ($P<0.05$), at week 4.

Table 2. Radiological findings for proximal and distal union at various postoperative intervals

Median (Range)				
Groups	Week 2	Week 4	Week 8	
			Proximal U.	Distal U.
A	0 (0-0)	0 (0-0)	0.5 (0-1)[@]	0 (0-1)
B	0 (0-0)	0 (0-0)	1 (0-1)[@]	1 (0-1)
C	0 (0-0)	0 (0-1)	1 (1-2)	1 (1-1)
D	0 (0-0)	0 (0-1)	1 (1-2)	1.5 (1-2)[*]
E	0 (0-0)	0 (0-1)	2 (1-2)	1.5 (1-2)[*]

- Symbol ([@]) shows significant difference in comparison with group E ($P<0.05$), for proximal union, at week 8.

Symbol (*) shows significant difference in comparison with group A ($P<0.05$), for distal union, at week 8.

Table 3. Radiological findings for remodeling over various postoperative intervals

Median (Range)			
Groups	Week 2	Week 4	Week 8
A	0 (0-0)	0 (0-0)	0 (0-0) [@]
B	0 (0-0)	0 (0-0)	0 (0-0) [@]
C	0 (0-0)	0 (0-0)	0 (0-0) [@]
D	0 (0-0)	0 (0-0)	0 (0-0) [@]
E	0 (0-0)	0 (0-0)	1 (0-1)

- Symbol ([@]) shows significant difference in comparison with group E ($P<0.05$), at week 8.

In week 4

The new bone formation activity was observed significantly more in the bone defect area of Groups D and E in comparison with Groups A and B (P<0.05). There were no significant differences in this parameter between Groups A and B (P>0.05), also between both control groups (A and B) and Group C (P> 0.05). The data showed that the bone formation score in Groups D and E was significantly more than Group C (P < 0.05), and there were no significant differences between Groups D and E (P>0.05; Table 1).

Our radiological evaluations showed that in week 4 minimum bone unity at the proximal and distal part of the defect happened in all treated groups, but there was no significant difference between them. We did not observe evidence of bone unity in control groups (A and B). Remodeling was not found in either group on the 28th day post-surgery (Tables 2 and 3).

In week 8

The investigation of radiographs of bone defects demonstrated that new bone formation was considerably developed in all tested groups. Our analysis of radiological data indicated that a significant difference was recorded only between Group E and control groups (A and B; P<0.05; Table 1).

Our study on radiographs showed that proximal bone unity in Group E was significantly more than the control groups (A and B; P<0.05), and there was no significant difference between the other groups (P>0.05). The evidence showed that there were significant differences in distal bone unity between Groups D and E in comparison with Group A (P<0.05; Table 2).

Remodeling was not found in all tested groups, except Group E on the 56th day post-surgery. Remodeling of the medullary canal (score 1) was seen in three of four animals in this group, which significantly was more than the other groups (P<0.05; Table 3).

In this study, the analysis of the total radiological point showed that in week 2, all treated groups significantly had a better score than Group A (P<0.05), and in week 4, Groups D and E significantly received a higher point compared to the control groups (A and B). Also, this point in Group E was significantly more than Group C (P<0.05). In week 8, all treated groups significantly had a better total radiological point compared with Group A (blank group); also, Group E was significantly better than Group B (P<0.05; Table 4 and Figure 1).

According to the results of this paper, based on Emery's microscopic and radiologic Lane and Sandhu scoring system, it could be concluded that separate or combined addition of human growth factor and PSCs to bone allograft had noticeably positive effects on the bone healing process, and it seems that combination therapy of the mentioned agents had a significant effect on the repair of the bone critical-size fracture.

Table 4. Findings for total radiological point over various postoperative intervals

Median (Range)			
Groups	Week 2	Week 4	Week 8
A	0 (0-1)	1 (1-1)$^{@\#}$	4 (4-4)
B	1 (1-1)*	1 (1-1)$^{@\#}$	4.5 (4-5)$^{@}$
C	1 (1-1)*	1 (1-4)$^{@}$	5 (5-7)*
D	1 (1-1)*	2 (1-4)	6 (5-8)*
E	1 (1-2)*	2 (2-4)	8.5 (5-9)*

- Symbol (*) shows significant difference in comparison with group A (P<0.05), at weeks 2 & 8.
- Symbol ($^{@}$) shows significant difference in comparison with group E (P<0.05), at weeks 4 & 8.
- Symbol ($^{\#}$) shows significant difference in comparison with group D (P<0.05), at week 4.

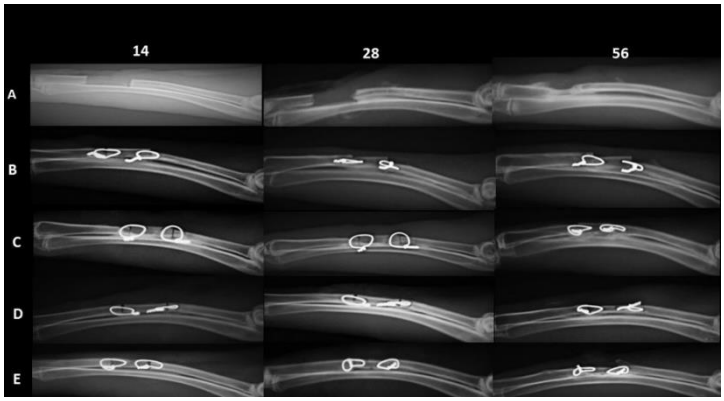

Fig. 1. Radiographs of the forelimb in control and treatment groups on the 14th, 28th, and 56th postoperative days.

Histological Analysis of Bone Regeneration

The histological evaluation of osteogenesis of bone regeneration of the five groups was carried out four and eight weeks after the radius CSD operation. Histological results revealed different bone regeneration results in the different groups.

Group A

In the blank control group (A), new bone was not found in the defect site four weeks postoperatively. The ingrowth of fibrous connective tissue over the empty defects was sparse. In longitudinal sections, the majority of the defect area was occupied by fibrous tissue except a few foci of fibro-cartilaginous transition zones (Figure 2, A1).

In eight weeks postoperatively, fibrous connective tissue was observed over the defects, and some woven bone had formed along the boundary of the bone defect. A large bone defect still remained in these two groups. Toluidine blue staining of the longitudinal section revealed only minimal mineralized areas, which are indicative of new bone formation (Figure 2, A2).

Group B

In contrast with the blank group (A), four weeks after surgery Masson's trichrome staining showed matrix collagen fibrils, and the new bone grew gradually from the bone defect boundary to the central area; inflammatory cell infiltration was not observed around the graft. Eight weeks after surgery, bridging callus or histological union did not develop in any of these defects, but some immature new bone formation was observed around both the end of the original radius (Figure 2, B).

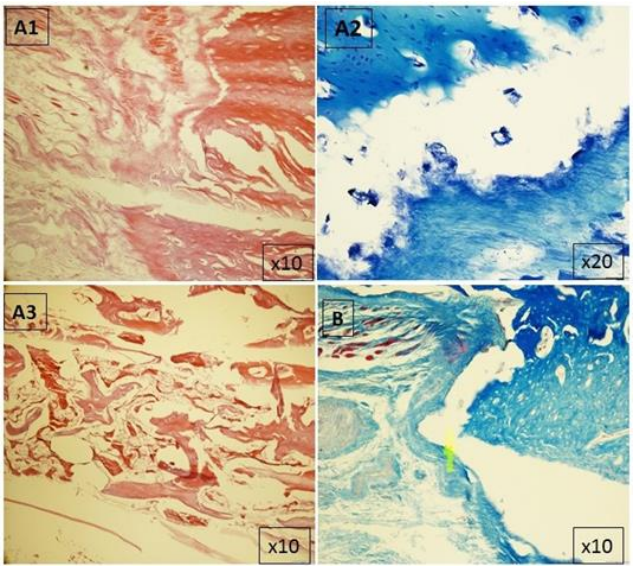

Fig. 2. Different types of tissue in the bone defect stained with H&E, toluidine blue, and Masson's trichrome.

Note. (A1): Well-organized fibrous scar tissue with the presence of blood vessels in week 4. (A2): Distinct boundary between the fibrocellular tissue and original bone end at graft site in week 8. (A3): Fibrous tissue mixing with dispersed lamellar bone in week 8. (B): In the control group, just fibrous scar replaced the graft defect in week 4.

Group C

Four weeks after surgery, the defect was almost filled by fibrocellular and fibrocartilage; compared to Group B, more new bone formation was observed. Some endosteal ossification inside the fibrocellular matrix was observed in the medulla of graft. Longitudinal sections stained with H&E showed the original radius periosteal extension into the radial defect area and formation of new bone (Figure 3, C1).

Eight weeks after surgery, the boundary between the graft and radius bone was filled by bone callus inside the fibrocartilage matrix. Granulation tissue is visible, and the overall shape of the bone graft was well maintained (Figure 3, C2).

Group D

After four weeks, endosteal and periosteal bones started to form; differentiation of fibroblast cells to cartilage and woven bone was visible (Figure 3, D1).

Eight weeks after surgery, the defect site was filled by bone callus and fibrocartilage tissue. There were not any signs of an inflammatory reaction to the graft in any cases of this group. Endosteal and periosteal bones were visible, such as new bone formation occurred via endochondral ossification (Figure 3, D2).

Group E

After four weeks, the defects were largely surrounded by callus and islands of woven bone, and bone formation was particularly advanced to the fracture borders. Further, the newly formed bone was found both in the center and boundary of the defect site with a wide distribution of the collagen fibrils of the matrix (Figure 4, E1).

After eight weeks postoperatively, the defect was filled by new bone. The newly formed bone almost had the same histological structure as normal bone. Remodeling of trabecular to compact bone was observed, along with intense vascularization, with

vessels being surrounded by calcified tissue, Haversian system, and Haversian canal, and lamellar bone was visible in this group. Marrow formation was evident in more than half of the implant areas indicative of remodeling. The graft was surrounded by or in contact with lamellar bone. No significant inflammatory response, necrosis or foreign body reactions were observed demonstrating good osteoconductive and biocompatibility (Figure 4, E2).

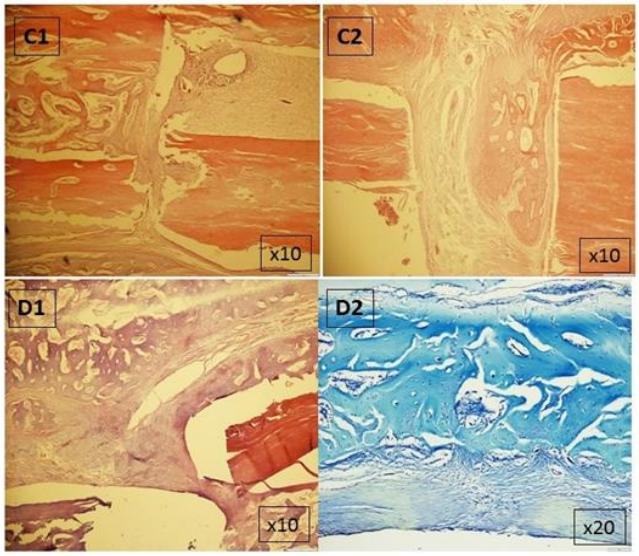

Fig. 3. Different types of tissue in the bone defect stained with H&E and toluidine blue.

Note. (C1): Small amounts of newly formed bone and large amounts of well-organized fibrous scar in week 4. (C2): Fibrous tissue and new bone were seen in junction of the boundary between the two at the graft site in week 8. (D1): Newly formed woven bone contains primarily newly formed bone near the graft and original bone in week 4 (D2): Lamellar bone, near the fibrocartilage tissue in week 8.

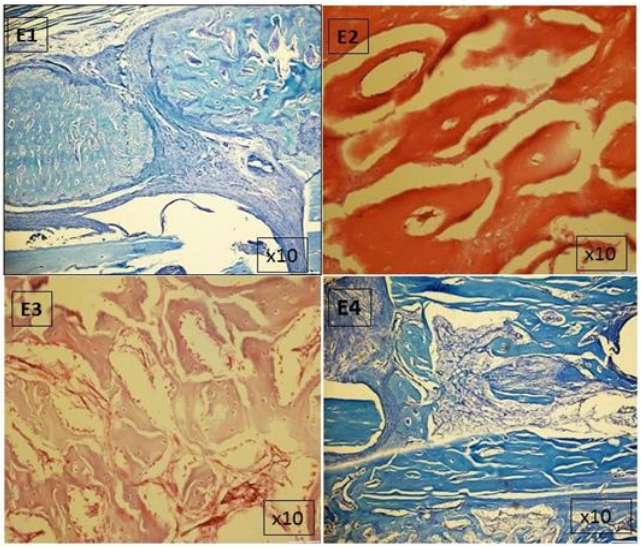

Fig. 4. The microscopic histological images of forelimb sections of Group E stained with H&E and toluidine blue.

Note. (E1): Large amounts of newly formed bone in the original defect with cartilage being the predominant tissue type found in the defect in week 4. (E2): Note to compact bone formation with several Haversian canals in week 8. (E3): Newly formed woven bone contains primarily new formed bone, fresh bone matrix, and osteoblast rim in week 8. (E4): New bone, occupied most of the original defect and marrow formation, was observed in the grafted area in week 8.

Statistical Analysis of Histopathological Evaluation

At week 4

The analysis of histopathologic scoring data showed that the bone healing process in defects of all treated groups (C, D, and E) was significantly more developed than the control groups (A and B; $P<0.05$). There was significantly more bone formation activity in the bone defects of Group B compared to Group A ($P<0.05$). A comparison of histological data between treated groups showed that the healing process in Group E significantly was in better condition than Group D ($P<0.05$; Table 5).

At week 8

The microscopic analysis of the healing process in bone defects of the treated groups (C, D, and E) revealed more advanced repair criteria than those of the control groups (A and B) significantly (P<0.05). There were no significant differences in histopathologic parameters between Groups A and B (P>0.05) and also between all the treated groups (P>0.05; Table 5).

Table 5. Finding based on pathological scoring system for evaluation of bone healing process at various postoperative intervals

Median (Range)		
Groups	Week 4	Week 8
A	2 (2-2)	3.5 (3-4)
B	3 (3-3)*	3.5 (3-5)
C	4.5 (4-5)$^{*\Phi}$	5.5 (5-6)$^{*\Phi}$
D	4 (4-5)$^{*\Phi@}$	5.5 (5-6)$^{*\Phi}$
E	5 (5-5)$^{*\Phi}$	6 (6-7) $^{*\Phi}$

- Symbol (*) shows significant difference in comparison with group A (P<0.05), at weeks 4 & 8.
- Symbol (Φ) shows significant difference in comparison with group B (P<0.05), at weeks 4 & 8.
- Symbol ($^{@}$) shows significant difference in comparison with group E (P<0.05), at week 4.

Discussion

The application of growth factors and stem cells for the osseous healing has been a subject of great interest for bone grafting. The purpose of our experimental study was to investigate the application of demineralized cortical bone graft seeded by allogeneic PSCs in combination with growth factors in rabbit with a skeletal CSD.

Extensive bone defects are more challenging to treat. In this regard, the healing rate depends on the size of the defect and the quality of the adjacent soft tissues. Large bone defects include segmental or critical size cortical defects, created by trauma, tumor resection, aseptic loosening around implants, and skeletal abnormality. CSD is defined as a defect with a minimum length that cannot be spontaneously treated, leading to non-union. Such defects are generally accepted to be ≥ 1.5 to two times the diameter of the long bone diaphysis, but they vary according to the host and bone (29,30).

Autologous bone grafting alone may be sufficient for bone defects that are no larger than 2–3 cm. In addition, because of quick graft resorption, cancellous bone grafting is frequently inappropriate for bone defects larger than 6 cm (31). Cortical allogeneic bone grafts exhibit excellent structural properties; however, because of a high susceptibility to infection, they are indicated specifically for defects without evidence of contamination, typically in post tumor reconstruction (32).

Decellularization of bone graft eliminates the immunogenicity and infectious risk associated with cortical bone allografts and, therefore, may be impressive in enhancing the solidarity of these grafts. Decellularization generally refers to the removal of non-extracellular matrix components, cells, cellular components, and other non-extracellular matrix components such as blood, antigens, serum, and fat (33). However, leaving intact an extracellular matrix component decellularized bone matrix is an allogeneic bone graft material, commonly used in orthopedics surgery for filling in boney defects after fractures, and has been widely used as a scaffold for bone tissue engineering because of its uniform structure and similarity to the original bone matrix, as well as its osteoconductive and biomechanical properties (34,35). Hashimoto Y *et al.* described that the decellularized bone graft also promoted the osteogenic differentiation of MSCs in vitro (36).

In this research, radiographic, gross, and histopathological observations showed that CSD remained unbridged with fibrous tissue proliferation and minimal new bone formation in control Group A with very slow progress in the healing rate. In Group B, radiographically, there was no close union between the construct and radius, but new bone formation at the defect initially occurred at both ends of the scaffolds and on the side of the scaffold adjacent to the radius and ulna. This is most probably because the proximal and distal ends of the scaffold were in contact with the bone marrow, which contains bone marrow stromal cells (BMSCs), and the side of the scaffold adjacent to the ulna was in contact with the periosteum, which contains osteoprogenitor cells.

Elimination of the periosteum severely restricts allograft healing because the periosteum is a vascularized tissue combined with an osteoconductive scaffold, osteoprogenitor cells, and osteoinductive factors, which interfere fracture healing and bone autograft incorporation (37). The development of tissue engineering techniques for the treatment of large bone defects enhances greater challenges. A complex method will be required to modify the healing process through seeded cell survival and to ensure prompt vessel ingrowth into the scaffold via a careful choice of structure and shape, together with the addition of cytokines and growth factors (38).

Thus, we hypothesize that a decellularized allogeneic bone tissue-engineered graft enriched with

periosteum derived stem cell and growth factors would provide sustained delivery of growth factors, support stem cell delivery, and improve allograft incorporation in a critical-sized rabbit radius defect. The positive effects of MSCs in the treatment of bone fractures have been demonstrated in several studies (39). Similarly, our results demonstrated that MSCs and cortical bone graft with or without platelet growth factors were effective in accelerating non-union bone fracture healing in rabbits. However, there are a few studies concluded that stem cells had no significant effects on the healing process of non-union bone fractures (40).

MSCs are well-known to have the potency to undergo osteogenic differentiation under optimal conditions. MSCs have the capacity to differentiate into osteoblasts and the possibility to transmit or release various conductive factors, which contribute to vessel and bone formation. The most commonly compared sources of mesenchymal progenitor cells are periosteal derived cells (PDC), synovium-derived cells (SDC), bone marrow-derived mesenchymal stromal cells (BM-MSC), muscle-derived cells (MDC), and adipose tissue-derived cells (ADC) (41,42). In an experimental study, Debnath *et al.* (2018) identified PSC that was present in the periosteum of long bones of mice, displayed clonal multipotency, and self-renewal properties. They show that PSCs display transcriptional signatures, which are distinct from those of other skeletal stem cells and mature mesenchymal cells. However, other skeletal stem cells form bone via an initial cartilage template using the endochondral pathway, PSCs form bone via a direct route, while other skeletal stem cells form bone via an initial cartilage template using the endochondral pathways (19).

Granero-Molto *et al.* and Undale *et al.* demonstrated that transplanted MSCs enhanced callus volume, increased new bone volume, and improved biomechanical properties and could induce fracture healing by increasing biomechanical properties in mice and non-union nude rat model (43, 44). Their proliferation and differentiation capacity may be elevated by exposing them to growth factors. Growth factors are protein signaling agents that release following injury, by bone lining cells, circulating platelets, and peripheral cell populations and act locally to stimulate formation and proliferation of osteoblasts and thereby promote bone healing (45).

Liu *et al.* (2007) demonstrated that bone morphogenetic protein-2 (BMP-2) has the greatest effect on the differentiation of MSCs to osteoblasts (46). Also, several studies have demonstrated the potency of the insulin-like growth factor (IGF) to elevate *in vivo* fracture healing (47). To determine the relevance of these findings for the clinical situation, we developed a large bone defect model in the rabbit. In this model, almost no bone unity was found in the defect site (over the course of eight weeks) when the defect was left empty, indicating that this model could be CSD. To test their bone repair potential, cells were seeded onto decellularized allogeneic bone graft and enriched by growth factors prior to implantation into the defects. When scaffolds (containing growth factors) were implanted, four weeks after surgery, bone formation was limited to the space of implanted graft medulla and most of bone union between the graft and radius was osteochondral type, as it was observed in the H&E stained sections. Eight weeks after surgery, the boundary between the graft and radius bone was filled by bone callus, and the longitudinal histopathological section from Group C showed a continuous pattern of bone formation in comparison to Groups B and E.

In Group D, the defect was implanted by graft enriched via periosteal stem cells four weeks after surgery, resulted in endosteal and periosteal bone formation; also, small islands of mature cartilage, undergoing replacement by bone, could still be found. Eight weeks after surgery, the longitudinal histopathological section showed that the defect site was filled by bone callus and fibrocartilage tissue. There were no signs of an inflammatory reaction to the scaffold and stem cells in any cases of this group. This faster healing potential noticed in Group D from gross, radiographic, and histopathological observations compared to Group B and blank group, which could be attributed to the osteogenic differentiation potential of periosteal derived stem cells.

Arinzeh *et al.* (2010) described that MSC therapy, in combination with an osteoconductive scaffold, is capable of regenerating bone in preclinical models of fracture healing (48). Ding *et al.* administered adipose stem cells and platelet-rich fibrin (PRF) to promote mandible defects in a dog. Similar to our results, they showed that proliferation and osteogenic potentials of stem cells were significantly enhanced by platelet growth factors (49). Oryan *et al.* (2018) demonstrated that the BMSCs have the potential to drastically increase the bone regeneration ability of osteoinductive scaffolds in critical-sized radial bone defects in rats (50). When the defect was filled by enriched graft with PSCs and growth factors in the treatment group, the histological section and radiology results from week 8 specimen showed that new bone formation and remodeling was underway in Group E. The defect was almost filled by new bone. Moreover, quantitative histological analyses did not confirm the quantitative differences in bone volume (new bone formation) between this group and the groups that treated with the scaffold enriched by growth factors and scaffold seeded by PSCs. However, they revealed that, when defects were implanted with this graft, the structural organization of the bone was restored and characterized by the full cortical bridging and reconstitution of the newly formed medullary canal with bone marrow, consisting of hematopoietic cells and adipocytes.

Furthermore, the Haversian system and Haversian canal are also visible in this group. No significant inflammatory response, necrosis, or foreign body reactions were observed, demonstrating good osteoconductive and biocompatibility of enriched graft. This better healing potential noticed in Group E based

on gross, radiographic, and histopathological observations, which could be attributed to the osteogenic differentiation potential of MSCs and osteoinductive effect of growth factors. Chan *et al.* confirmed the positive effects of a combination of growth factor and BMSCs on the bone healing process; they reported that growth factor encourages the osteoinductive activity of bone marrow activity to improve bone healing (51).

In bone union, MSCs play an important role in the bone regenerative mechanism. Granero-Molto *et al.* and Undale *et al.* reported that transplanted MSCs enhanced callus volume, increased new bone volume, and improved biomechanical properties and could induce fracture healing by increasing biomechanical properties in mice and non-union nude rat model (52). Romero *et al.* also described the potential of growth factor and MSCs to stimulate the healing process and new bone formation in a critical-sized mouse femur defect without inflammatory response to the graft (53). The outcome of our study is in agreement with the above-mentioned researches that declare PSC seeded in bone allograft enriched by human growth factors, which could accelerate the formation of bone callus at the fracture gap in rabbit radial CSD.

There are some limitations in this study, which should be addressed in future research. First, in order to evaluate the therapeutic activity of stem cells, cell tracking techniques are required to determine the fate of transplanted cells in the healing tissue of the fracture site. Second, in order to more precise evaluation of quality and quantity of callus formation in the fracture site, usage of the computed tomography (CT) scan technique could be suitable for future studies.

Conclusion

Based on the results of this study, it appears that implantation of concentrated PSCs in combination with growth factors and allogeneic cortical bone graft is an effective therapy for the repair of the large bone defect. Our results also show that engineering bone allografts can improve the delivery of exogenous cells to the defect site without causing chronic inflammation.

Acknowledgements

This work was supported financially by a Grant for Scientific Research from Vice-Chancellor of Research of Shahid Bahonar University of Kerman, Iran.

Conflict of Interest

The authors declared that there is no conflict of interest regarding the publication of this article.

References

1. Schindeler A, McDonald MM, Bokko P, Little DG. Bone remodeling during fracture repair: The cellular picture. In Seminars in cell & developmental biology 2008 Oct 1 (Vol. 19, No. 5, pp. 459-466). Academic Press. [DOI:10.1016/j.semcdb.2008.07.004] [PMID]
2. Frolke JP, Patka P. Definition and classification of fracture non-:union:s. Injury. 2007; 38(Suppl. 2):19-22. [DOI/10.1016/S0020-1383(07)80005-2]
3. Killington K, Mafi R, Mafi P, Khan WS. A systemic review of clinical studies investigating mesenchymal stem cells for fracture non-:union: and bone defects. Current stem cell res. & therapy sur. 2018 May 1;13(4):284-91. [DOI:10.2174/1574888X12666170915121137] [PMID]
4. Reed AA, Joyner CJ, Brownlow HC, Simpson AH. Human atrophic fracture non-:union:s are not avascular. J Orthop Res. 2002 May;20(3):593-9. [DOI:10.1016/S0736-0266(01)00142-5]
5. Bishop JA, Palanca AA, Bellino MJ, Lowenberg DW. Assessment of compromised fracture healing. J Am Acad Orthop Surg. 2012 May 1;20(5):273-82. [DOI:10.5435/JAAOS-20-05-273] [PMID]
6. Robinson CM, McQueen MM, Wakefield AE. Estimating the risk of non:union: following nonoperative treatment of a clavicular fracture. J Bone Joint Surg Am. 2004 Jul 1;86(7):1359-65. [DOI:10.2106/00004623-200407000-00002] [PMID]
7. Rosenberg GA, Sferra JJ. Treatment strategies for acute fractures and non:union:s of the proximal fifth metatarsal. J Am Acad Orthop Surg. 2000 Sep 1;8(5):332-8. [DOI:10.5435/00124635-200009000-00007] [PMID]
8. Yellowley C. CXCL12/CXCR4 signaling and other recruitment and homing pathways in fracture repair. Bonekey Rep. 2013; 2. [DOI:10.1038/bonekey.2013.34] [PMID] [PMCID]
9. Malhotra A, Pelletier MH, Yu Y, Walsh WR. Can Platelet-rich plasma (PRP) improve bone healing? A comparison between the theory and experimental outcomes. Arch. Of ortho And trauma Surg. 2013 Feb 1;133(2):153-65. [DOI:10.1007/s00402-012-1641-1] [PMID]
10. Nandi SK, Roy S, Mukherjee P, Kundu B, De DK, Basu D. Orthopaedic applications of bone graft & graft substitutes: a review. Indian J Med Res. 2010; 132(1):15-30.
11. Brydone AS, Meek D, Maclaine S. Bone grafting, orthopaedic biomaterials, and the clinical need for bone engineering. Proceedings of the Institution of Mechanical Engineers, Part H: Proc Inst Mech Eng H. 2010 Dec; 224(12):1329-43. [DOI:10.1243/09544119JEIM770] [PMID]
12. Lohmann CH, Andreacchio D, Köster G, Carnes Jr DL, Cochran DL, Dean DD, Boyan BD, Schwartz Z. Tissue response and osteoinduction of human bone grafts in vivo. Arch Orthop Trauma Surg. 2001 Nov 1;121(10):583-90. [DOI:10.1007/s004020100291] [PMID]
13. Pokorny JJ, Davids H, Moneim MS. Vascularized bone graft for scaphoid non:union:. Tech Hand Up Extrem Surg. 2003 Mar 1;7(1):32-6. [DOI:10.1097/00130911-200303000-00007] [PMID]
14. Bigham-Sadegh A, Karimi I, Alebouye M, Shafie-Sarvestani Z, Oryan A. Evaluation of bone healing in canine tibial defects filled with cortical autograft, commercial-DBM, calf fetal DBM, omentum and omentum-calf fetal DBM. J Vet Sci. 2013; 14(3):337-343. [DOI:10.4142/jvs.2013.14.3.337] [PMID] [PMCID]
15. Elder BD, Eleswarapu SV, Athanasiou KA. Extraction techniques for the decellularization of tissue engineered

articular cartilage constructs. Biomaterials. 2009 Aug 1;30(22):3749-56. [DOI:10.1016/j.biomaterials.2009.03.050] [PMID] [PMCID]

16. Vavken P, Joshi S, Murray MM. TRITON-X is most effective among three decellularization agents for ACL tissue engineering. J Orthop Res. 2009 Dec;27(12):1612-8. [DOI:10.1002/jor.20932] [PMID] [PMCID]
17. Zhang AY, Bates SJ, Morrow E, Pham H, Pham B, Chang J. Tissue engineered intrasynovial tendons: optimization of acellularization and seeding. J Rehabil Res Dev. 2009;46(4):489-98. [DOI:10.1682/JRRD.2008.07.0086] [PMID]
18. Gui L, Chan SA, Breuer CK, Niklason LE. Novel utilization of serum in tissue decellularization. Tissue Eng Part C Methods. 2010 Apr;16(2):173-84. [DOI:10.1089/ten.tec.2009.0120] [PMID] [PMCID]
19. Bahney CS, Zondervan RL, Allison P, Theologis A, Ashley JW, Ahn J, Miclau T, Marcucio RS, Hankenson KD. Cellular biology of fracture healing. J Orthop Res. 2019 Jan;37(1):35-50. [DOI:10.1002/jor.24170] [PMID] [PMCID]
20. Debnath S, Yallowitz AR, McCormick J, Lalani S, Zhang T, Xu R, Li N, Liu Y, Yang YS, Eiseman M, Shim JH. Discovery of a periosteal stem cell mediating intramembranous bone formation. Nature. 2018 Oct;562(7725):133-9. [DOI:10.1038/s41586-018-0554-8] [PMID] [PMCID]
21. Yang JW, Park HJ, Yoo KH, Chung K, Jung S, Oh HK, Kim HS, Kook MS. A comparison study between periosteum and resorbable collagen membrane on iliac block bone graft resorption in the rabbit calvarium. Head Face Med. 2014 Dec;10(1):15. [DOI:10.1186/1746-160X-10-15] [PMID] [PMCID]
22. Janicki P, Schmidmaier G. What should be the characteristics of the ideal bone graft substitute? Combining scaffolds with growth factors and/or stem cells. Injury. 2011; 42:77-81. [DOI:10.1016/j.injury.2011.06.014] [PMID]
23. Zimmermann G, Moghaddam A. Allograft bone matrix versus synthetic bone graft substitutes. Injury. 2011; 42:16-21. [DOI:10.1016/j.injury.2011.06.199] [PMID]
24. Toosi S, Behravan N, Behravan J. Non:union: fractures, messenchymal stem cells and bone tissue engineering. J Of Biomed Material Res Part A. 2018 Sep; 106(9):2552-62. [DOI:10.1002/jbm.a.36433] [PMID]
25. Wise DL. Preclinical evaluation of bone graft substitutes. In: Bensen CV, An YH, Friedman RJ, editors. Biomat and bioeng handbook. New York: CRC Press. 2000; 699-716.
26. Oryan A, Alidadi S, Bigham-Sadegh A, Moshiri A: Healing potential of polymethylmethacrylate bone cement combined with platelet gel in the critical-sezed radial bone defect of rats. J Plos One. 2018; 13(4):e0194751 [DOI:10.1371/journal.pone.0194751] [PMID] [PMCID]
27. Emery SE, Brazinski MS, Koka A, Bensusan JS, Stevenson s. The biological and biomechanical effects of irradiation on anterior spinal bone grafts in a canine model. J Bone Joint Surg Am. 1994; 76(4): 540-8. [DOI:10.2106/00004623-199404000-00008] [PMID]
28. Shafiei Z, Bigham AS, Dehghani SN, Nezhad ST: Fresh cortical autograft versus fresh cortical allograft effects on experimental bone healing in rabbits: radiological, histopathological and biomechanical evaluation. Cell Tissue Bank. 2009; 10:19-26. [DOI:10.1007/s10561-008-9105-0] [PMID]
29. Gugala Z, Lindsey RW, Gogolewski S. New approaches in the treatment of critical-size segmental defects in long bones. Macromol Symp. 2007; 253:147-161 [DOI:10.1002/masy.200750722]
30. Sato K, Watanabe Y, Harada N, et al. Establishment of reproducible, critical-sized, femoral segmental bone defects in rats. Tissue Eng Part C Methods. 2014; 20:1037 [DOI:10.1089/ten.tec.2013.0612] [PMID]
31. Meesters DM, Wijnands KA, Brink PR, Poeze M. Malnutrition and Fracture Healing: Are Specific Deficiencies in Amino Acids Important in Non:union: Development. Nutrients. 2018 Nov;10(11):1597. [DOI:10.3390/nu10111597] [PMID] [PMCID]
32. Cooper GM, Mooney MP, Gosain AK, Campbell PG, Losee JE, Huard J. Testing the critical size in calvarial bone defects. revisiting the concept of a criticalsize defect. Plast Reconstr Surg. 2010; 125:1685 [DOI:10.1097/PRS.0b013e3181cb63a3] [PMID] [PMCID]
33. Beno T, Yoon YJ, Cowin S, et al. Estimation of bone permeability using accurate microstructural measurements. J Biomech. 2006; 39:2378-2387. [DOI:10.1016/j.jbiomech.2005.08.005] [PMID]
34. Pisetsky DS. DNA and the immune system. Ann Intern Med 1997; 126:169-171. [DOI:10.7326/0003-4819-126-2-199701150-00015] [PMID]
35. Mygind T, StiehlerM, Baatrup A, Li H, Zou X, Flyvbjerg A, et al. Mesenchymal stem cell ingrowth and differentiation on coralline hydroxyapatite scaffolds. Biomaterials. 2007; 28:1036-47. [DOI:10.1016/j.biomaterials.2006.10.003] [PMID]
36. Hashimoto Y, Funamoto S, Kimura T, et al. The effect of decellularized bone/bone marrow produced by high-hydrostatic pressurization on the osteogenic differentiation of mesenchymal stem cells. Biomaterials. 2011; 32:7060-7067. [DOI:10.1016/j.biomaterials.2011.06.008] [PMID]
37. Allen MR, Hock JM, Burr DB. Periosteum: biology, regulation, and response to osteoporosis s therapies. Bone. 2004; 35(5):1003-12. [DOI:10.1016/j.bone.2004.07.014] [PMID]
38. Petite H, Vandamme K, Monfoulet L, Logeart-Avramoglou D. Strategies for improving the efficacy of bioengineered bone constructs: a perspective. Osteoporos Int. 2011; 22:2017-21. [DOI:10.1007/s00198-011-1614-1] [PMID]
39. Mousaei Ghasroldasht M, Matin MM, Kazemi Mehrjerdi H, Naderi-Meshkin H, Moradi A, Rajabioun M, Alipour F, Ghasemi S, Zare M, Mirahmadi M, Bidkhori HR. Application of mesenchymal stem cells to enhance non-:union: bone fracture healing. J Of Biomed Material Res Part A. 2019 Feb;107(2):301-11. [DOI:10.1002/jbm.a.36441] [PMID]
40. Dozza B, Salamanna F, Baleani M, Giavarei G, Parrilli A, Zani L, e, al. Non:union: fracture healing: Evaluation of effectiveness of demineralized bone matrix and mesenchymal stem cells in novel sheep bone non:union:

model. J of tissue eng and reg med. 2018 Sep;12(9)1972-85 [DOI:10.1002/term.2732] [PMID]

41. Jaiswal N, Haynesworth SE, Caplan AI, et al. Osteogenic differentiation of purified, culture-expanded human mesenchymal stem cells in vitro. J Cell Biochem. 1997; 64:295-312. https://doi.org/10.1002/(SICI)1097-4644(199702)64:2<295::AID-JCB12>3.0.CO;2-I [DOI:10.1002/(SICI)1097-4644(199702)64:23.0.CO;2-I]

42. Pittenger MF, Mackay AM, Beck SC, et al. Multilineage potential of adult human mesenchymal stem cells. Science. 1999; 284:143-7. [DOI:10.1126/science.284.5411.143] [PMID]

43. Granero-Molto F, Weis JA, Miga MI, et al. Regenerative effects of transplanted mesenchymal stem cells in fracture healing. Stem Cells. 2009; 27:1887-98. [DOI:10.1002/stem.103] [PMID] [PMCID]

44. Undale A, Fraser D, Hefferan T, et al. Induction of fracture repair by mesenchymal cells derived from human embryonic stem cells or bone marrow. J Orthop Res. 2011; 29:1804-11. [DOI:10.1002/jor.21480] [PMID] [PMCID]

45. Dequeker J, Mohan S, Finkelman RD, Aerssens J, Baylink DJ. Generalized osteoarthritis associated with increased insulin-like growth factor types I and II and transforming growth factor beta in cortical bone from the iliac crest. Possible mechanism of increased bone density and protection against osteoporosis. Arthr Rheum. 1993; 36:1702-8. [DOI:10.1002/art.1780361209] [PMID]

46. Liu Y, Huse R O, de Groot K, Buser D, Hunziker E B. Delivery mode and efficacy of BMP-2 in association with implants. J Den. Res. 2007; 86:84-89. [DOI:10.1177/154405910708600114] [PMID]

47. Schmidmaier G, Wildemann B, Stemberger A, Haas NP, and Raschke M. Biodegradable poly(D,L- lactide) coating of implants for continuous release of growth factors. J Biomed Mater Res Appl Biomat. 2001; 58:449-455. [DOI:10.1002/jbm.1040] [PMID]

48. Arinzeh TL, Peter SJ, Archambault MP, van den Bos C, Gordon S, Kraus K, et al. Allogeneic mesenchymal stem cells regenerate bone in a critical-sized canine segmental defect. J Bone Joint Surg Am. 2003; 85:1927-35. [DOI:10.2106/00004623-200310000-00010] [PMID]

49. Ding L, Tang S, Liang P, Wang C, Zhou Pf, Zheng L. Bone Regeneration of Canine Peri-implant Defects Using Cell Sheets of Adipose-Derived Mesenchymal Stem Cells and Platelet-Rich Fibrin Membranes. J Oral Maxillofac Surg, 2019; 77:499-514. [DOI:10.1016/j.joms.2018.10.018] [PMID]

50. Oryan A, Baghaban Eslaminejad M, Kamali A, Hosseini S, Moshiri A, Baharvand H. Mesenchymal stem cells seeded onto tissue-engineered osteoinductive scaffolds enhance the healing process of critical-sized radial bone defects in rat. Cell and Tissue Res. 2018;734: 63-81 [DOI:10.1007/s00441-018-2837-7] [PMID]

51. Chen X, Wang J, Yu L, Zhou J, Zheng D and Zhang B. Effect of concentrated growth factor (CGF) on the promotion of osteogenesis in bone marrow stromal cells (BMSC) in vivo. Sci Rep. 2018; 8: 5876. [DOI:10.1038/s41598-018-24364-5] [PMID] [PMCID]

52. Granero-Molto F, Weis JA, Miga MI, et al. Regenerative effects of transplanted mesenchymal stem cells in fracture healing. Stem Cells. 2009; 27:1887-98. [DOI:10.1002/stem.103] [PMID] [PMCID]

53. Romero R, Travers JK, Asbury E, Pennybaker A, Chubb L, et al. Combined delivery of FGF-2, TGF-β1, and adipose-derived stem cells from an engineered periosteum to a critical-sized mouse femur defect. 2017; 105A:900-911. [DOI:10.1002/jbm.a.35965] [PMID]

How to Cite This Article

Hassibi, H., Farsinejad, A., Dabiri, S., Vosough, D., Mortezaeizadeh, A., Kheirandish, R., Azari, O. Allogenic Bone Graft Enriched by Periosteal Stem Cell and Growth Factors for Osteogenesis in Critical Size Bone Defect in Rabbit Model: Histopathological and Radiological Evaluation. *Iranian Journal of Pathology*, 2020; 15(3): 205-216. doi: 10.30699/ijp.2020.101715.2013